Article

Importance of Fuel Cell Tests for Stability Assessment—Suitability of Titanium Diboride as an Alternative Support Material

Christina Roth [1,*]**, Peter Bleith** [2]**, Christoph A. Schwöbel** [3]**, Sebastian Kaserer** [3] **and Jens Eichler** [4]

[1] Physikalische und Theoretische Chemie, Freie Universität Berlin, Berlin 14195, Germany
[2] Paul Scherrer Institut, Villigen 5232, Switzerland; E-Mail: peter.bleith@psi.ch
[3] Institute for Materials Science, Technische Universität Darmstadt, Darmstadt 64289, Germany;
    E-Mails: schwoebel@fm.tu-darmstadt.de (C.A.S.); kaserer@energy.tu-darmstadt.de (S.K.)
[4] ESK Ceramics GmbH und Co. KG, Kempten 87437, Germany;
    E-Mail: Jeichler@mmm.com

* Author to whom correspondence should be addressed; E-Mail: Christina.Roth@fu-berlin.de;
    Tel.: +49-30-8385-0960; Fax: +49-30-8385-4792.

Abstract: Carbon corrosion is a severe issue limiting the long-term stability of carbon-supported catalysts, in particular in the highly dynamic conditions of automotive applications. (Doped) oxides have been discussed as suitable alternatives to replace carbon, but often suffer from poor electron conductivity. That is why non-oxide ceramics, such as tungsten carbide and titanium nitride, have been discussed recently. Titanium diboride has also been proposed, due to its promising activity and stability in an aqueous electrochemical cell. In this work, Pt nanoparticles were deposited onto μm-sized TiB_2 particles with improved grain size, manufactured into porous gas diffusion electrodes and tested in a realistic polymer electrolyte membrane (PEM) fuel cell environment. In contrast to the model studies in an aqueous electrochemical cell, in the presence of oxygen and high potentials at the cathode side of a real fuel cell, TiB_2 becomes rapidly oxidized as indicated by intensely colored regions in the membrane-electrode assembly (MEA). Moreover, already the electrode manufacturing process led to the formation of titanium oxides, as shown by X-ray diffraction measurements. This demonstrates that Cyclic Voltammetry (CV) measurements in an aqueous electrochemical cell are not sufficient to prove stability of novel materials for fuel cell applications.

---

1. Introduction

Polymer electrolyte membrane (PEM) fuel cells certainly are a viable way towards clean and efficient energy conversion, in particular, when hydrogen from renewable sources is utilized. With numerous prospective stationary, mobile and portable applications, their broad commercialization, however, has not yet taken place. This is mainly due to their high cost and limited durability. Corrosion of the carbonaceous support materials is a severe drawback, since it will lead to the loss of electrode porosity and eventually of Pt nanoparticles and thus catalytically active surface. That is why the search for novel and more durable support materials as an alternative to the currently-applied high-surface area carbons is a very active field of research.

Both electron conducting polymers and oxides have been proposed in the literature, such as polyaniline [1–4], doped titanium oxides [5–8] and doped tin oxides [9,10]. But while these materials often show promising stabilities, their electron conductivities are comparatively low. And because of their low surface area, they cannot easily be manufactured into porous electrodes [11]. Ways to prevent these drawbacks are the fabrication of composite electrodes, as shown exemplary by Ma *et al.* [12], Kakaei [13], and Lee *et al.* [14], or the use of advanced fabrication techniques adapted to the specifics of the new materials, such as electrospinning of polymer-oxide mixtures [15].

Non-oxide ceramics are another group of materials, which seem fit to replace the commonly applied carbonaceous supports. Important compounds of this group, which show both electrical conductivity and high chemical and thermal stability, are tungsten carbide, titanium nitride and titanium diboride [16–19]. Decorated with Pt nanoparticles, all of them have demonstrated sufficient catalytic activity for the relevant electrochemical oxygen reduction reaction (ORR) at the fuel cell cathode. Moreover, their stability at high potentials significantly surpassed the stability of carbon-supported nanoparticles.

However, one general shortcoming in the investigation of novel materials for fuel cell cathodes is that the tailored catalysts are often only tested in an aqueous electrochemical cell in acidic media. While this set-up allows for well-defined testing conditions with the catalyst's situation largely comparable to real-life studies, effects induced by subjecting the electrocatalyst to an oxygen atmosphere at the cathode side may be missed. The same is true for changes introduced by the flow of current between the electrodes [20].

In 2010, Mu *et al.* [21] described the application of TiB_2 as a possible support material for stable fuel cell catalysts for the first time. In their paper, they presented remarkable stability data in an accelerated stress test (AST). After 6000 cycles between 0 V and 1.2 V *vs.* reversible hydrogen electrode (RHE) the loss of electrochemically active surface was four times less than for the standard Pt/C catalyst, although the dispersion of the Pt nanoparticles on the support grains required improvement. In 2011, the same group presented a more successful synthesis pathway for Pt nanoparticles on TiB_2 using Nafion™ ionomer as both surfactant and stabilizer for an improved dispersion [19]. The results by Yin *et al.* [19] demonstrated an enhanced interaction between the

Nafion-stabilized Pt nanoparticles and the non-oxide ceramic support. In addition to the catalyst's excellent thermal stability and electrical conductivity, the ORR activity was comparable to the state-of-the-art Pt on carbon fuel cell catalyst.

In the present work, TiB_2-supported Pt nanoparticles for application at the cathode side of H_2/O_2 PEM fuel cells were synthesized using the method by Yin *et al.* [19]. Since the primary particle size of the TiB_2 is of importance for the final electrode fabrication and structuring, the TiB_2 synthesis route was modified to obtain support grains with sizes in the 0.1–10 μm range. This is not an easy task, as small particles are easily inflammable. X-ray diffraction (XRD) and transmission electron microscopy (TEM) were applied to reveal crystalline phases, platinum particle size and dispersion. X-ray diffraction was also used to follow changes in the crystalline part of the support material during electrode preparation and fuel cell testing. To determine the catalyst's activity and stability cyclic voltammetry (CV) tests in an aqueous electrochemical cell were applied. Furthermore, the catalyst powders were prepared into inks, airbrushed onto a Nafion™ membrane and tested in a realistic PEM fuel cell environment. The latter was done to show that CV tests in aqueous electrochemical cells are not sufficient to indicate the stability of a novel material for fuel cell applications. Though time-consuming and tedious, it is required to also investigate the material's behavior in a realistic fuel cell under operating conditions.

2. Experimental

2.1. TiB₂ Support Materials

Synthesis of the TiB_2 powder was done by carbothermal reduction of titanium dioxide powder (TiO_2—anatas structure, D50 = 0.68 μm) using boron carbide powder (B_4C, D50 = 5.83 μm) and carbon (C—Carbon Black, D50 = 3.14 μm). A variation of the synthesis parameters, such as composition and furnace parameters, was necessary in order to produce support particles with reduced sizes. The goal was to be comparable with the standard carbon support material.

The carbothermal reduction reaction is a two-step process, as was confirmed by X-ray diffraction and previously described by Baca *et al.* [22]:

$$TiO_2 + B_4C + C \rightarrow TiBO_3 + C \rightarrow TiB_2$$
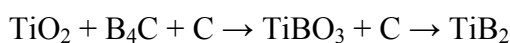
TiO_2 (63.2 wt%) was mixed in ethanol with 22.3 wt % B_4C and 14.5% C. The powder mixture was stirred and ultrasonicated to achieve good homogeneity. After drying at 75 °C for 8 h the mixture was heat-treated in a graphite furnace. The furnace was heated with constant power of 5 kW until 1050 °C, followed by a 200 K/h ramp up to 1400 °C and a holding time of one hour. The powder was jet milled (Noll GmbH, Bobingen, Germany) with a sifter cut off grain size of 6 μm (maximum particle size). Particle size distributions for raw as well as final powder were measured using a Mastersizer 2000 (Malvern Instruments Ltd., Malvern, Worcestershire, UK). The final TiB_2 powder has a D50 size fraction with a particle size of 1.5 μm.

2.2. Platinum Deposition on TiB$_2$

Platinum nanoparticles were deposited according to a process described by Yin *et al.* [19]. TiB$_2$ powder (200 mg) was dispersed in 10 mL ethanol with the supersonic disintegrator Vibra Cell 75Q4 (Fisher Scientific, Schverte, Germany) at 21% of the maximum amplitude. Ultrasound was applied for 4 s and paused for 2 s, followed by 4 s of ultrasonic treatment *etc.* (henceforth called 04/02-mode). 300 mL ethanol, 300 mL MilliQ water and 2.5 mL Nafion™ solution were put into a round bottom flask and stirred. The TiB$_2$ dispersion was added drop wise into this solution. The final suspension was stirred for another 3 h in order to obtain Nafion™-covered TiB$_2$ particles. 180 mg H$_2$PtCl$_6$ were added subsequently. This resulted in a decrease in the pH value to 2–3. Adding 1 M sodium hydroxide solution raised the pH to a suitable value of 9, which is in the optimum range for Pt nanoparticle synthesis. This mixture was then refluxed for 1.5 h at 80 °C. After cooling, the obtained catalyst was filtered and dried over night at 80 °C in a drying oven.

2.3. Physical Characterization

Physical characterization of the samples with respect to Pt nanoparticle size, particle dispersion and crystalline phases was performed by X-ray powder diffraction and transmission electron microscopy. X-ray powder diffraction (XRD) measurements were carried out with a STOE STADI-P diffractometer (STOE und CIE GmbH, Darmstadt, Germany) using germanium monochromized Mo K$_{\alpha 1}$ radiation (λ = 0.71069 Å). To determine the average crystallite size of the platinum particles, Rietveld refinement using the FULLPROF software package [23] was performed.

Transmission electron microscopy (TEM) was carried out using a FEI CM20 (FEI Deutschland GmbH, Frankfurt, Germany) operating at 200 kV acceleration voltage with a LaB$_6$ filament. For sample preparation, a small amount of the powder catalyst was dispersed in ethanol using ultrasound and one drop was transferred to a standard holey carbon film-covered copper grid. Particle sizes were estimated using the semi-automated software LINCE [24].

2.4. Electrochemical Characterization

2.4.1. Cyclic Voltammetry (CV)

Electrochemical characterization was carried out first using cyclic voltammetry with a VMP2 multichannel potentiostat (Princeton Applied Research, AMETEK GmbH, Meerbusch, Germany). The reference electrode was a standard calomel electrode (SCE) with a potential of +0.241 V *vs.* normal hydrogen electrode (NHE). As electrolyte 0.1 M perchloric acid was used and purged with nitrogen for at least 10 min in order to remove traces of oxygen from the solution. For each sample, 10 mg catalyst powder were mixed with 1 mL MilliQ water and dispersed for 10 min. in 04/02-mode with the supersonic finger. 20 µL of this dispersion was applied on a polished glassy carbon disk electrode (7 mm in diameter). After drying at 80 °C, 200 µg of the catalyst remained on the electrode tip. Base voltammogramms were obtained with a scan rate of 30 mV/s, before 1 M methanol was added to the electrolyte and the methanol oxidation activity recorded. Accelerated stress tests (AST) similar to the ones reported by [19] were carried out for all samples (not shown).

2.4.2. MEA Preparation and Fuel Cell Test

In addition to the electrochemical characterization by cyclic voltammetry, current-voltage characteristics were recorded in a realistic fuel cell set-up. Membrane-electrode assemblies (MEA) consisting of an activated Nafion™ membrane with one electrode on each side were fabricated by an adapted airbrush technique. The ink used for the anode was prepared from 200 mg Pt/C catalyst mixed with 2.66 mL MilliQ water, 1.33 mL Nafion™ and 12 mL ethanol. For the cathode, Nafion™ ionomer was replaced by MilliQ water, because the cathode catalyst already contained Nafion™ (ref. synthesis method [19]). The ink was dispersed by ultrasonic treatment for 10 min in 04/02-mode. The ink was applied onto the membrane heated to 90 °C by a slightly modified airbrush technique using Eco spray containers resulting in an approx. Pt loading of 0.8 mg·cm^{-2} per electrode. A spraying mask restricted the area of the electrodes to a square of 5×5 cm. The ink was applied in successive layers, which were left to dry on the heated vacuum table. The final MEA was then assembled, put into the commercially available fuel cell hardware from Electrochem Inc. (Woburn, MA, USA), and mounted into the home-made fuel cell test bench. Gas diffusion layers (Toray paper, SGL Carbon SE, Wiesbaden, Germany) were placed on each side of the MEA and topped with bipolar plates and so-called pin-type flow fields. The cell was heated to 70 °C with the anode humidifier set to 90 °C. The gas flow was set to 60 mL·min^{-1} oxygen and 120 mL·min^{-1} hydrogen, as only the anode feed was humidified. The current-voltage characteristics (E-i curve) were recorded starting from the highest possible cell current, reducing it stepwise to 0 and back to the maximum value, but without a systematic and tedious optimization of operating conditions (flows, T, humidification, back pressure) to obtain the maximum cell performance possible. The cells were operated for at least 3 days each (up to 200 cycles), whilst repeatedly recording E-i curves.

3. Results and Discussion

Nafion™-stabilized Pt nanoparticles on TiB$_2$ were synthesized by Yin *et al.* [19] synthesis and their structure investigated using XRD and TEM. Figure 1 shows the diffraction pattern of the Pt nanoparticle decorated catalyst. The typical pattern of hexagonal titanium diboride is observed with sharp reflections in good agreement with grain sizes in the μm-range. After Pt nanoparticle decoration additional broad reflections typical of nm-sized fcc Pt appear. Rietveld refinement estimates an average Pt nanoparticle size of ≈5 nm.

Figure 2 shows a transmission electron micrograph of the Pt-decorated titanium diboride support material. Nafion™-stabilized Pt nanoparticles can only be imaged at the edges of the μm-sized TiB$_2$ support grains. The support appears dark, as the electrons cannot penetrate through the thick material in the grain center. In higher resolution, the nanoparticles appear to be coated with a polymer film. The observed size of the Pt particles is in good agreement with the estimated value from X-ray diffraction measurements.

Figure 1. X-ray diffraction pattern of Pt nanoparticles supported on TiB₂. Both measured data and Rietveld refinement are shown. Sharp reflections belong to the support material, broad reflections can be attributed to the Pt nanoparticles. The Pt nanoparticle size is ≈5 nm.
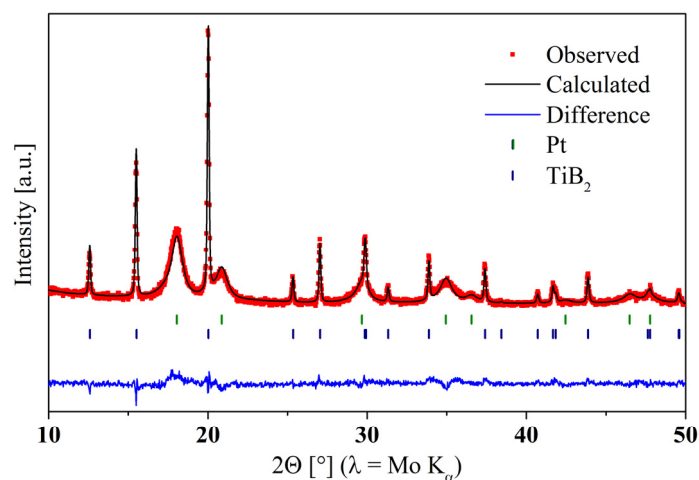

Figure 2. Transmission electron micrograph of Pt/TiB₂. Nafion™-stabilized Pt nanoparticles can only be imaged in thinner edge regions, as the μm-sized TiB₂ grains are too thick to let electrons pass through the grain center. The average Pt particle size as *ca.* 5 nm embedded in a Nafion™ ionomer film.
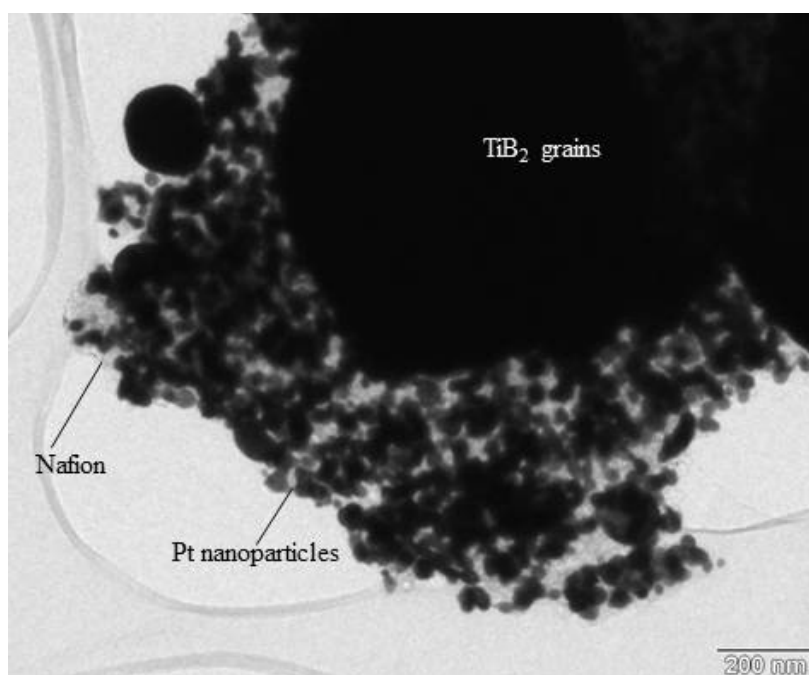
As in previous works by Yin *et al.* [19] cyclic voltammetry was applied to assess the electrocatalytic activity and stability of the catalysts. Figure 3a shows a base voltammogram of Pt/TiB₂ with the characteristic hydrogen and oxygen adsorption regions, which can be used to estimate the electrochemically active surface area (ECSA). In Figure 3b, the activity of the Pt nanoparticles for methanol oxidation is demonstrated, indicating that the active Pt surface is not covered by strongly adsorbed impurities from the synthesis procedure and can be accessed sufficiently by reactants. Methanol was used as a probe molecule, as in contrast to the (for a cathode catalyst) more appropriate

oxygen reduction reaction the electrode porosity only plays a minor role. Accelerated stress tests in an electrochemical cell (not shown) were in good agreement with literature data. Carbon-supported Pt loses ≈ 50% of its electrochemically active surface area (ECSA) during the stress test, whereas the ECSA of Pt/TiB$_2$ is only reduced by 1/3. However, a direct comparison is not easily possible, as the ECSA of the titanium boride-supported sample is much lower already at the beginning.

Figure 3. (**a**) Base voltammogram of a Pt/TiB$_2$ catalyst in 0.1 M perchloric acid showing the prominent Pt characteristics. Different sweeps are presented showing the loss of ECSA with extended cycling up to 100 cycles; (**b**) cyclic voltammogram of the same Pt/TiB$_2$ catalyst in 1 M methanol solution as a reliable activity probe (black—second cycle, blue—10th cycle).


(**a**)

(**b**)
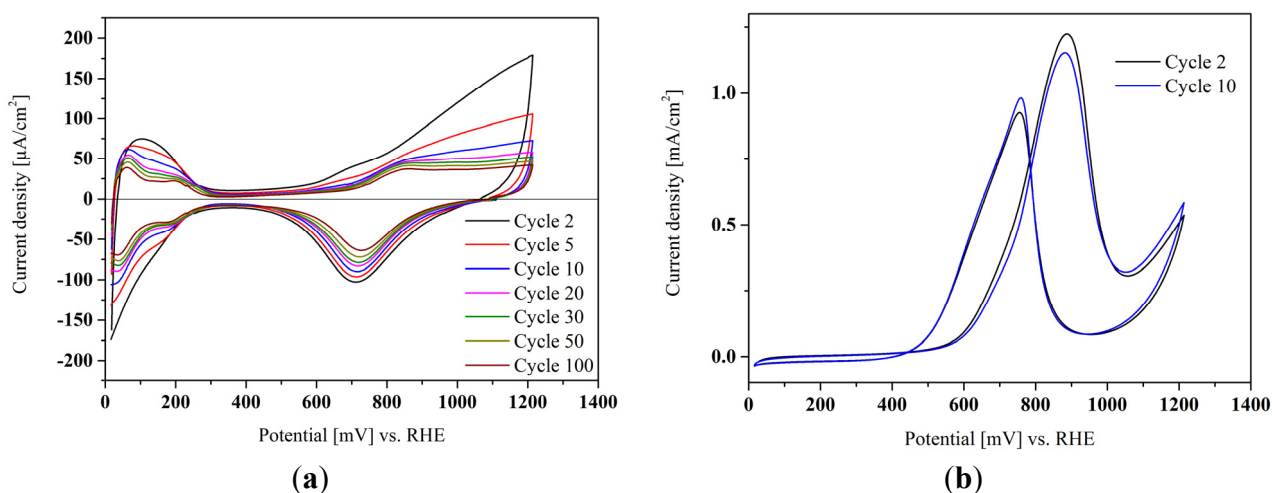
As pointed out in the Introduction section, though helpful for a first assessment of catalytic activity and stability, cyclic voltammetry and accelerated stress tests in an aqueous environment do not take into account the presence of oxygen at the cathode side and also not the elevated temperatures of 80 °C instead of room temperature. That is why we fabricated the Pt/TiB$_2$ electrocatalyst powder into an ink and sprayed porous electrodes for fuel cell tests in a more realistic environment. In Figure 4, X-ray diffraction patterns of the as-synthesized Pt/TiB$_2$ powder (Figure 4, bottom), of the powder scratched off directly after electrode preparation and no fuel cell test (Figure 4, middle) and of the electrocatalyst scratched off from the electrode after extended fuel cell testing (Figure 4, top) are compared. While the pattern of the as-synthesized powder can be fitted by plain TiB$_2$, in the other two data sets additional reflections appear. A particularly dominant peak is attributed to the (211) reflection of TiO$_2$ in its rutile structure. Part of the non-oxide support is already converted into a titanium oxide by the spraying process, before it is even tested in a fuel cell. Surface oxidation may take place due to the contact with Nafion™ at elevated temperatures. Compared to the standard Pt/C cathode catalyst, the novel Pt/TiB$_2$ catalyst does not perform well in fuel cell tests. This could be due to an excess of Nafion™ ionomer from the catalyst synthesis, but also to the not-yet optimized fuel cell testing conditions. Current-voltage characteristics show a power maximum of max. 40 mW·cm^{-2}, in contrast to 160 mW·cm^{-2} for the Pt-on-carbon reference measurement. After a short conditioning period, where the current increases, probably due to an increased hydration and thus improved proton conduction of the membrane, the cell's power output declines steadily (Figure 5). This may be correlated with the structural changes in the electrode, such as the oxidation of the support, which can also be seen in scanning electron

micrographs before and after operation (Figure 5). In particular, the electron conductivity of titanium sub-oxides may be significantly lowered as compared to TiB_2.

Figure 4. Diffraction patterns of Pt/TiB_2 powder as-synthesized (**bottom**), after preparation into a porous electrode with no fuel cell operation (**middle**), after fuel cell operation (**top**). While the as-synthesized support can be described by pure TiB_2, the other diffraction patterns display an additional peak of the TiO_2 rutile phase. TiB_2 already starts to oxidize during the electrode fabrication step.
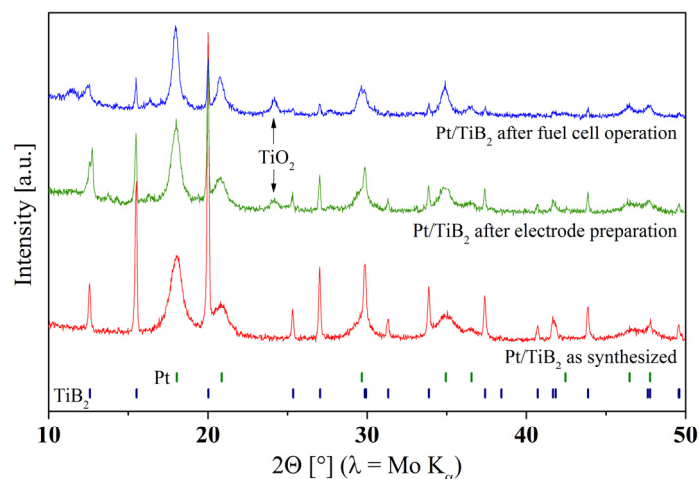
Figure 5. Decline of power output during fuel cell operation and comparison of the corresponding SEM images before and after operation.
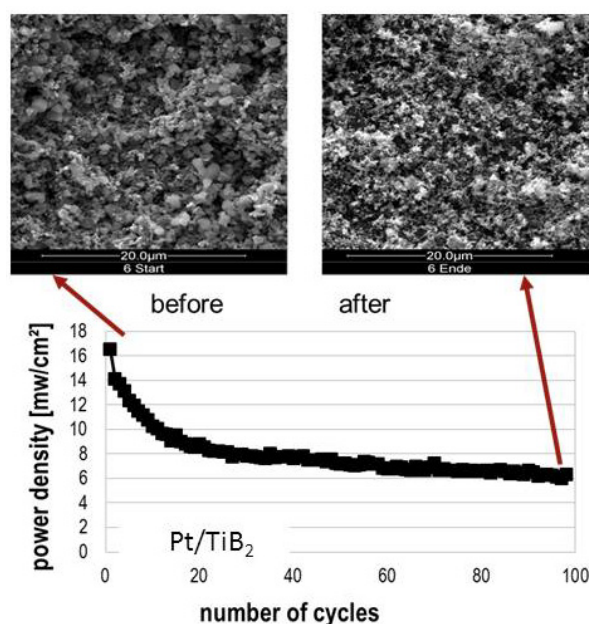

After operation in a fuel cell for at least 3 days and repeatedly taking E-i curves, the MEA was recovered and analyzed. Significant coloring of the previously black electrode can be observed already with the naked eye (Figure 6). Lustrous blue, green and orange colors appear across the electrode indicating the formation of titanium oxides, either different phases or thicknesses. The most intense blue color can be seen close to the oxygen inlet, while the color changes to orange closer to the oxygen

outlet. Obviously, most of the titanium diboride support has been transformed into titanium oxides in the presence of oxygen and high potentials at the cathode side. And the different colouring may also trace the cathode flow field and indicate oxygen starvation along the way.

Figure 6. Photograph of TiB$_2$ electrode after fuel cell test. Iridescent blue regions close to the oxygen inlet (**top left**) indicate where titanium diboride has been transformed into titanium oxide. At the oxygen outlet (**bottom right**), orange colors dominate.
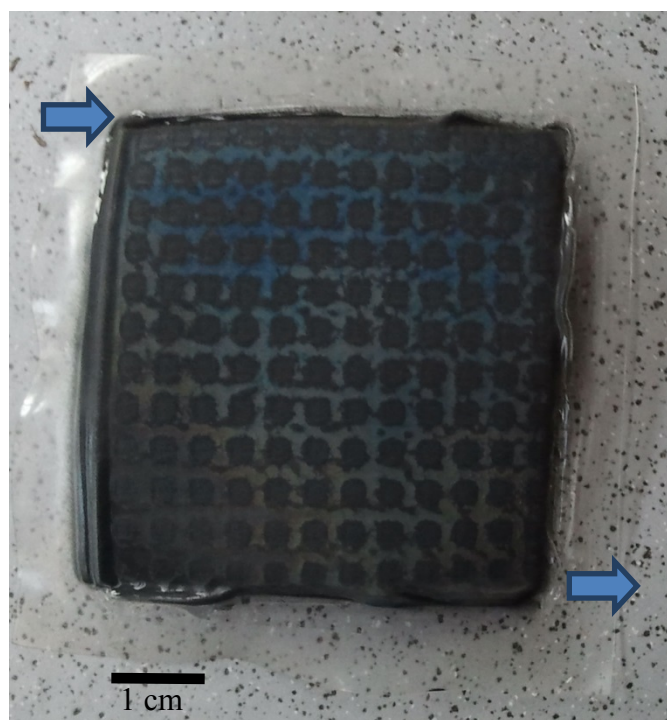
4. Conclusions

TiB$_2$ was tested as an alternative material to replace the standard carbon support, which is prone to corrosion. Pt nanoparticles of about 5 nm in size were homogeneously distributed on the μm-sized support grains, which were obtained by an improved synthesis pathway. A variation of the synthesis parameters was necessary in order to produce smaller grain sizes, which are comparable with the standard carbon support material. The catalyst yielded high activity and stability when tested by cyclic voltammetry, in good agreement with the literature. However, in a realistic fuel cell set-up the presence of oxygen and high potentials at the cathode side led to a conversion of the titanium diboride into titanium oxides. This process was directly visible by a color change of the MEA from blue close to the oxygen inlet to orange close to the oxygen outlet. Surface oxidation already took place during the electrode fabrication step by airbrushing and proceeded further during fuel cell operation, as indicated by SEM images taken before and after fuel cell operation as well as the decline in power output. Ti oxides will be less electron-conducting than TiB$_2$, thus significantly impacting the fuel cell performance. These results underline the importance of realistic fuel cell tests for the reliable stability assessment of novel materials.

Acknowledgments

Author Contributions

Christina Roth is head of the research group, in which the work was carried out. She supervised this study and wrote most of the manuscript. Jens Eichler is employed by ESK Advanced Ceramics GmbH and responsible for the collaboration. He synthesized the various TiB$_2$ supports and developed synthesis strategies to reduce their aggregate size. Peter Bleith and Christoph Schwöbel are the two students responsible for the synthesis of the Pt supported catalysts and involved in their electrochemical analysis. Sebastian Kaserer supported the students during the electrochemical testing and contributed the structural characterization by X-ray diffraction, SEM and TEM.

Conflicts of Interest

The authors declare no conflict of interest.

References

1. Antolini, E.; Gonzalez, E. Polymer supports for low-temperature fuel cell catalysts. *Appl. Catal. A* **2009**, *365*, 1–19.
2. Carmo, M.; Roepke, T.; Roth, C.; dos Santos, A.M.; Poco, J.G.R.; Linardi, M. A novel electrocatalyst support with proton conductive properties for polymer electrolyte membrane fuel cell applications. *J. Power Sources* **2009**, *191*, 330–337.
3. Wang, Y.-J.; Wilkinson, D.P.; Zhang, J. Non-carbon support materials for polymer electrolyte fuel cell electrocatalysts. *Chem. Rev.* **2011**, *111*, 7625–7651.
4. Sharma, S.; Pollet, B.G. Support materials for PEMFC and DMFC electrocatalysts—A review. *J. Power Sources* **2012**, *208*, 96–119.
5. Gustavsson, M.; Ekstrom, H.; Hanarp, P.; Eurenius, L.; Lindbergh, G.; Olsson, E.; Kasemo, B. Thin film Pt/TiO$_2$ catalysts for the polymer electrolyte fuel cell. *J. Power Sources* **2007**, *163*, 671–678.
6. Huang, S.Y.; Ganesan, P.; Popov, B.N. Titania supported platinum catalyst with high electrocatalytic activity and stability for polymer electrolyte membrane fuel cell. *Appl. Catal. B* **2011**, *102*, 71–77.
7. Ioroi, T.; Siroma, Z.; Fujiwara, N.; Yamazaki, S.I.; Yasuda, K. Sub-stoichiometric titanium oxide-supported platinum electrocatalyst for polymer electrolyte fuel cells. *Electrochem. Commun.* **2005**, *7*, 183–188.
8. Rajalakshmi, N.; Lakshmi, N.; Dhathathreyan, K.S. Nano titanium oxide catalyst support for proton exchange membrane fuel cells. *Int. J. Hydrog. Energy* **2008**, *33*, 7521–7526.
9. Chhina, H.; Campbell, S.; Kesler, O. An oxidation-resistant indium tin oxide catalyst support for proton exchange membrane fuel cells. *J. Power Sources* **2006**, *161*, 893–900.

10. Lee, K.S.; Park, I.S.; Cho, Y.H.; Jung, D.S.; Jung, N.; Park, H.Y.; Sung, Y.E. Electrocatalytic activity and stability of Pt supported on Sb-doped SnO_2 nanoparticles for direct alcohol fuel cells. *J. Catal.* **2008**, *258*, 143–152.

11. Ettingshausen, F.; Suffner, J.; Kaserer, S.; Hahn, H.; Roth, C. Sb-Doped SnO_2 hollow spheres offering Micro- and Nanoporosity in fuel cell electrode structures. *Adv. Energy Mater.* **2011**, *1*, 648–654.

12. Ma, J.; Habrioux, A.; Guignard, N.; Alonso-Vante, N. Functionalizing effect of increasingly graphitic carbon supports on carbon-supported and TiO_2-Carbon composite-supported Pt nanoparticles. *J. Phys. Chem. C* **2012**, *116*, 21788–21794.

13. Kakaei, K. Electrochemical characteristics and performance of platinum nanoparticles supported by Vulcan/Polyaniline for oxygen reduction in PEMFC. *Fuel Cells* **2012**, *12*, 939–945.

14. Lee, J.M.; Han, S.B.; Kim, J.Y.; Lee, Y.W.; Ko, A.R.; Roh, B.; Hwang, I.; Park, K.W. TiO_2@carbon core-shell nanostructure supports for platinum and their use for methanol electrooxidation. *Carbon* **2010**, *48*, 2290–2296.

15. Cavaliere, S.; Subianto, S.; Savych, I.; Jones, D.J.; Roziere, J. Electrospinning: Designed architectures for energy conversion and storage devices. *Energy Environ. Sci.* **2011**, *4*, 4761–4785.

16. Shen, P.K.; Yin, S.; Li, Z.; Chen, C. Preparation and performance of nanosized tungsten carbides for electrocatalysis. *Electrochim. Acta* **2010**, *55*, 7969–7974.

17. Chhina, H.; Campbell, S.; Kesler, O. Thermal and electrochemical stability of tungsten carbide catalyst supports. *J. Power Sources* **2007**, *164*, 431–440.

18. Avasarala, B.; Murray, T.; Li, W.; Haldar, P. Titanium nitride nanoparticles based electrocatalysts for proton exchange membrane fuel cells. *J. Mater. Chem.* **2009**, *19*, 1803–1805.

19. Yin, S.; Mu, S.; Pan, M.; Fu, Z. A highly stable TiB_2-supported Pt catalyst for polymer electrolyte membrane fuel cells. *J. Power Sources* **2011**, *196*, 7931–7936.

20. Roth, C.; Ramaker, D.E. Operando XAS techniques: Past, present, future. In *Fuel Cell Science*; Wieckowski, A., Ed.; Wiley-VCH: Weinheim, Germany, 2010; pp. 511–544.

21. Mu, S. Fuel Cells Durability and Performance. In Proceedings of the 6th Fuel Cells Durability Conference, Boston, MA, USA, 9–10 December 2010.

22. Baca, L.; Stelzer, N. Adapting of sol-gel process for preparation of TiB_2 powder from low-cost precursors. *J. Eur. Ceram. Soc.* **2008**, *28*, 907–911.

23. Roisnel, T.; Rodríguez-Carvajal, J. WinPLOTR: A Windows tool for powder diffraction pattern analysis. *J. Mater. Sci. Forum* **2001**, *378*, 118–123.

24. Dos Santos e Lucato, S.L. LINCE V2.42. Ph.D. Thesis, Materials Science Department, TU Darmstadt, Karolinenplatz, Darmstadt, Germany, 1999.